Analyst

PAPER

View Article Online
View Journal | View Issue

Cite this: *Analyst*, 2018, **143**, 150

Towards the electrochemical diagnostic of influenza virus: development of a graphene–Au hybrid nanocomposite modified influenza virus biosensor based on neuraminidase activity†

Ülkü Anik, *[a] Yudum Tepeli,[a] Maher Sayhi,[b,c] Jihene Nsiri[b] and Mohamed Fethi Diouani*[b]

Received 15th September 2017,
Accepted 25th October 2017

DOI: 10.1039/c7an01537b

rsc.li/analyst

An effective electrochemical influenza A biosensor based on a graphene–gold (Au) hybrid nanocomposite modified Au-screen printed electrode has been developed. The working principle of the developed biosensor relies on the measurement of neuraminidase (N) activity. After the optimization of experimental parameters like the effect of bovine serum albumin addition and immobilization times of fetuin A and PNA lectin, the analytical characteristics of the influenza A biosensor were investigated. As a result, a linear range between 10^{-8} U mL^{-1} and 10^{-1} U mL^{-1} was found with a relative standard deviation value of 3.23% (for 10^{-5} U mL^{-1} of N, *n*:3) and a limit of detection value of 10^{-8} U mL^{-1} N. The developed biosensor was applied for real influenza virus A (H9N2) detection and very successful results were obtained.

Introduction

The influenza virus A can be described as a negative stranded RNA virus which belongs to the *Orthomyxoviridae* family. The virus contains two surface glycoproteins namely hemagglutinin (H) and neuraminidase (N). The classification of the virus subtype can be made according to the antigenic properties of these 18 H (1–18) and 11 N (1–11) glycoproteins.[1–14] Since the influenza virus is very mutagenic, it can easily change the antigenic portions of H and N proteins and as a result a very serious antigenic drift has occurred.[15] Seasonal influenza viruses can easily be affected by these antigenic drift mutations which cause millions of serious infections and approximately 500 000 deaths every year.[15,16] Also, sometimes two or more influenza A viruses of different origin infect the same cell and as a result, new strains or subtypes emerge because of the occurrence of genetic reassortment.[1] As an example, the reassortment between human and avian virus strains was the reason for the influenza A pandemics in 1957 (H2N2) and in 1968 (H3N2) while in 2009 the (H1N1) pandemic virus was found to be a reassortment containing gene segments from human, avian and swine influenza viruses.[2,4] Besides these, highly mortal avian viruses like H5N1 and H7N9 have been found to transmit from birds to humans.[4,17] Because of these, some researchers define the virus as causing "continuously emerging influenza disease" which means it still continues to be a threat for animals and human beings.[15]

Although rapid detection of influenza virus is mandatory, present diagnostic techniques cannot compete with the mutagenic behavior of the virus. For example, viral culture, which has been accepted as a golden standard method, needs two or three days to retrieve the results which is a somewhat long time for the diagnosis of the influenza virus.[18–20] On the other hand, quantitative polymerase chain reaction (qPCR), which is chosen frequently by health personnel, can be described as sensitive but relatively slow (about 2 h) method for influenza detection. qPCR is also expensive and can be performed only by specialists.[20–22] Apart from these methods, various immune based rapid tests have been fabricated recently to compensate the need for the fast diagnosis of the virus. From this point of view, these tests manage to show the results in 15 to 30 min. However, they lack the sensitivity and the precision.[20,21,23,24]

Electrochemical techniques are accepted as practical techniques for many applications.[25,26] The combination of electrochemical techniques with biosensor systems results in electrochemical biosensors which provide not only practicality but also selectivity and sensitivity.[27,28] For these reasons, electrochemical biosensors can be accepted as good candidates to be used in point of care systems.[29] Recently electrochemical bio-

[a]*Mugla Sitki Kocman University, Faculty of Science, Chemistry Department, Kotekli/Mugla, Turkey. E-mail: ulkuanik@mu.edu.tr*
[b]*Laboratory of Epidemiology and Veterinary Microbiology (LEMV), Institut Pasteur de Tunis, University of Tunis El Manar, LR11IPT03, Tunis-Belvédère 1002, Tunisia. E-mail: fethi.diouani@pasteur.rns.tn*
[c]*Faculty of Sciences of Tunis, University of Tunis El Manar, Tunisia*

†Electronic supplementary information (ESI) available. See DOI: 10.1039/c7an01537b

sensors were combined with nanomaterials and as a result, more sensitive and accurate results were obtained.[30–32] Graphene is a kind of two-dimensional nanomaterial and provides properties like higher surface area and good conductivity which are very important for electrochemical biosensors.[33–35] Apart from graphene, recently graphene–metallic nanocomposites were produced and used in these systems. These nanocomposites provide more sensitive and selective results when combined with the biosensor systems.[36–43]

Considering the influenza biosensors, it can be stated that, until now almost only H based systems have been developed.[7–10,44–48] Lately our group managed to develop a N based electrochemical influenza biosensor.[14] In that work, as preliminary data, only the electrochemical impedance spectroscopy (EIS) diagrams of the fabrication of a biosensor were presented.[14] For that earlier work, a glassy carbon paste electrode was used as the main electrode. First fetuin A which is a kind of glycoprotein, was attached onto the electrode. Then, N was immobilized onto fetuin A. Fetuin A includes terminal 12–14 sialic acid residues per molecule and N cleaves fetuin A from these sialic acid ends. Lastly, peanut agglutinin (PNA) lectin was immobilized onto the electrode surface to monitor this cleavage.[14]

In this work, as a continuation of our previous paper, we improve our system by using a gold screen-printed electrode (AuSPE) together with a graphene–Au hybrid nanocomposite. Also the experimental parameters of the developed system were optimized and the analytical characteristics were examined. Lastly, the developed biosensor was applied for real influenza A virus (H9N2) detection.

Experimental

Chemicals

Graphite powder, $NaNO_3$, chloroauric acid ($HAuCl_4{\cdot}H_2O$), $K_3[Fe(CN)_6]$, $K_4[Fe(CN)_6]{\cdot}3H_2O$, *N*-(3-dimethylaminopropyl)-*N*′-ethylcarbodiimide hydrochloride (EDC), *N*-hydroxysuccinimide (NHS), fetuin A, bovine serum albumin (BSA), N, PNA lectin, MES monohydrate and ethylene glycol (EG) were purchased from Sigma-Aldrich. H_2SO_4, H_2O_2, $KMnO_4$, KH_2PO_4, NaOH, NaCl and KCl were obtained from Merck. Double distilled water was used for the preparation of all solutions. All chemicals were of analytical grade and were used without needing further purification.

Instrumentation

Electrochemical measurements were carried out by using μ-AUTOLAB Type III with the FRA 2 module electrochemical measurement system from Metrohm B.V. that is controlled by NOVA 1.10 software. AuSPE was used as a working electrode and was purchased from Dropsens. SEM and EDS measurements were performed using a JSM-7600 F FEG-SEM at 15.0 kV. During the preparation procedure of a graphene–Au nanocomposite, a Thermo Electron Corporation pH-meter, an IKA ® C-MAG HS7 hotplate, a Bandelin Sonorex sonicator and a NUVE vacuum oven were used. For the incubation of biological materials at 37 °C an incubator shaker was used. ELLA measurements were carried out using an automatic plate reader with a 490 nm filter.

Synthesis procedure of graphene–Au nanocomposite

In order to synthesize a graphene–Au nanocomposite, graphene oxide (GO) was used as the starting material. Therefore, first GO was synthesized from graphite by using a modified Hummers–Offeman method.[38,49] For this purpose, 1 g of graphite powder was added into 23 mL of 98% H_2SO_4 solution and stirred at room temperature for 24 h. Then, 100 mg of $NaNO_3$ was added into the mixture and stirred for another 30 min. After the mixture was cooled to 5 °C by using an ice-bath, 3 mg of $KMnO_4$ was added to the medium and then the stirred mixture was heated up to 40 °C. 46 mL of double distilled water was added into the above mixture for a period of 25 min. Finally, 140 mL of double distilled water and 10 mL of 30% H_2O_2 were added into the mixture to stop the reaction. The unexploited graphite in the resulting mixture was removed by centrifugation. Then the mixture was dried in a desiccator at room temperature.

Additionally, for the graphene–Au nanocomposite synthesis step, a 10 mg portion of GO powder which was synthesized by using the modified Hummers–Offeman method was dispersed in 10 mL of water by sonication for 1 h to form a stable GO colloid.[50,51] Then, 20 mL of EG solution and 0.5 mL of 0.01 M $HAuCl_4{\cdot}H_2O$ were added to the GO colloid and stirred for 30 min. After that, the mixture was heated at 100 °C for 6 h by applying magnetic stirring. Subsequently, the graphene–Au nanocomposites were separated from the EG solution *via* centrifugation and washed with deionized water five times. The resulting product was dried in a vacuum oven at 60 °C for 12 h.[37] Finally, the synthesized graphene–Au nanocompsite was dispersed to 10 mg mL^{-1} in double distilled water by ultrasonication and stored at 4 °C until it was used.[38,40,41,52]

Preparation of developed electrochemical influenza A biosensor

AuSPE was used as the supporting electrode for the preparation of the developed electrochemical influenza A biosensor. First, AuSPE was modified with a graphene–Au hybrid nanocomposite. For this purpose, 6 μL of graphene–Au nanocomposite dispersion (10 mg mL^{-1}, in double distilled water) was dropped onto the surface of AuSPE and dried at room temperature for 1 h. Then, 10 μL of a 50 mM EDC/NHS mixture (in 50 mM MES pH: 5.5 solution) was dropped onto the electrode surface and left for 1 h. Subsequently, the electrode surface was rinsed with MES and phosphate buffered saline (PBS) with a pH value of 7.4 (137 mM NaCl, 10 mM KH_2PO_4, and 2.7 mM KCl). After that, 10 μL of 250 μg/250 μL of fetuin A in 0.1 M PBS was immobilized onto the electrode surface and left for 30 min. The electrode surface was then washed with PBS and then 10 μL of 1% BSA (in 0.1 PBS) solution was dropped onto the electrode surface for performing BSA effect experiments. Other than that, BSA was not used

during the fabrication of the influenza A virus biosensor. After that, the electrode was rinsed with PBS and 10 μL of different concentrations of N (in 0.1 M pH: 7.4 PBS) was dropped onto the electrode surface and kept for 18 h at 37 °C under stirring. After the electrode surface was washed with PBS, 10 μL of 50 μg mL^{-1} PNA lectin (in 0.1 M pH: 7.4 PBS) solution was dropped onto the developed electrochemical biosensor for 1 h at +4 °C. PNA lectin here specifically binds to the galactose molecules that appear after N cleaves the sialic acids from the fetuin A molecule. In this way, the N activity of the developed influenza A biosensor was determined electrochemically (Scheme 1). The characterization of the developed electrochemical influenza A biosensor and the determination of N activity studies were carried out by using the EIS method.

Influenza type A virus replication in embryonated eggs

H9N2 influenza type A virus (A/Equi/1/Prague 56) was propagated in 11-day old specific-pathogen free (SPF) chicken embryonated eggs *via* the allantoic route. The eggs were incubated at 37 °C for three days and the allantoic fluid was collected, and clarified by centrifugation at 3000*g* for 15 min. The viral titer, in the collected allontoic fluids, was monitored by performing a hemagglutination test.

ELLA measurements

An Enzyme-Linked Lectin Assay (ELLA) was performed to measure influenza A virus N activity as described by Couzens, L. *et al.*[3] A fetuin-coated plate was prepared by dispensing 100 μl per well of 25 μg ml^{-1} fetuin working solution into each well. The plate was covered and placed at +4 °C for 24 hours. Then, the plate was washed 3 times with 200 μl per well PBS wash buffer for 3 minutes. 100 μl sample diluent buffer was added in column 12 as a negative control and 50 μl serial dilution antigen (influenza virus, N and non-infected allantoic fluid) was transferred from the dilution plate to each well in columns 1–11 of the fetuin-coated plate containing an equal volume of the sample diluent buffer. The plate was incubated in a humidified incubator with 5% CO_2 for 18 hours at 37 °C, and then washed 6 times as described before. 100 μl per well PNA-peroxidase was dispensed into each well and incubated at room temperature for 2 hours. After this step, 3 time wash was performed before the addition of 100 μl per well freshly prepared substrate solution for 10 min in the dark at room temperature. The color reaction was stopped by the addition of 100 μl per well stop solution. The plates were read at 490 nm using a 96-well automatic plate reader.

Results and discussion

Characterization of synthesized graphene–Au hybrid nanocomposite

Fig. 1 shows the SEM images and EDS results of the graphene–Au nanocomposite. It can be seen from Fig. 1 that AuNps are located on the graphene sheets as white dots (average diameter of 250 nm). EDS results show that the atomic dispersion percentages of the graphene–Au nanocomposite are 83.73%, 14.97%, and 1.06% and the mass percentages of these elements are 69.29%, 14.66% and 14.32% for C, O and Au, respectively.

Electrochemical characterization of developed electrochemical influenza A biosensor

The fabrication of the developed influenza A biosensor was monitored *via* EIS in the presence of 10 mM $K_3[Fe(CN)_6]/K_4[Fe(CN)_6]$. From the Nyquist plots of EIS (Fig. 2), it can be seen that bare AuSPE has a small semi-circle domain because of the high conductivity of the Au surface (curve a). After the electrode modification with the graphene–Au hybrid nanocomposite, the semi-circle domain increases a little bit (curve b). After that, when the electrode surface was covered with fetuin A, the resistance of the electrode surface increased since the active surface area was blocked (curve c). Then, N was immobilized on to fetuin A from the sialic acid sides. Therefore, the electrode surface was covered with N and the charge transfer ability of the electrode surface was reduced

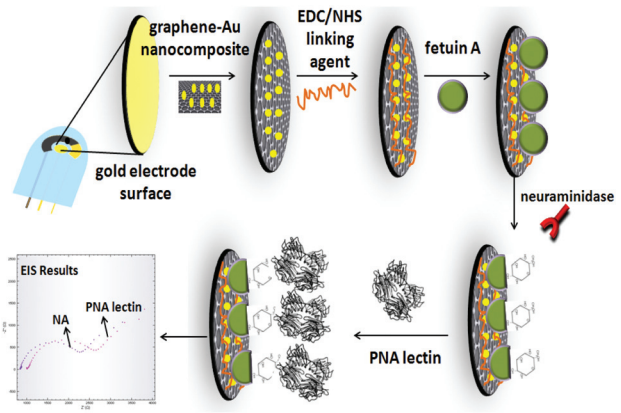

Scheme 1 Schematic diagram depicting the steps of the developed electrochemical influenza A biosensor.

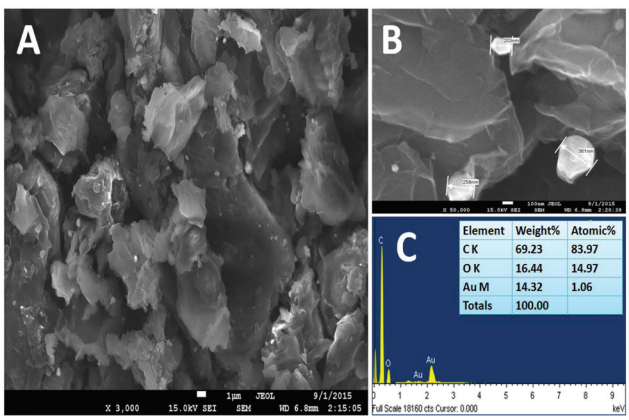

Fig. 1 (A), (B) SEM images of a graphene–Au nanocomposite and (C) EDS results of the graphene–Au nanocomposite.

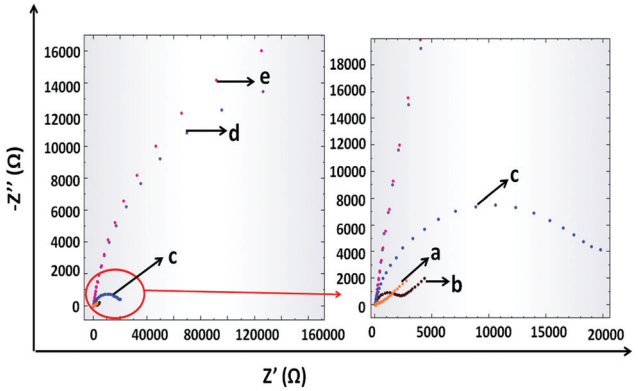

Fig. 2 Nyquist plots of the developed influenza A viral biosensor. a. Plain AuSPE, b. AuSPE/graphene-AuNp, c. AuSPE/graphene-AuNp/fetuin A, d. AuSPE/graphene-AuNp/fetuin A/N, and e. AuSPE/graphene-AuNp/fetuin A/N/PNA lectin. The EIS procedure was set to measure the electron transfer resistance in the frequency range of 0.1 Hz–10 kHz at a potential of 0.1 V and 10 mM $K_3[Fe(CN)_6]/K_4[Fe(CN)_6]$ (in pH: 7.4, 0.1 M PBS) was used as a redox probe.

resulting in the increment in the semicircle diameter (curve d). Lastly, PNA lectin, which shows specificity to galactose molecules that appear after the cleavage of fetuin A with N, was used. When the PNA lectin binds onto the galactose molecules, the electron transfer gets even tougher and the semicircle diameter also increases due to the resistance increase on the electrode surface (curve e).

Optimization of experimental parameters

The experimental parameters consisting of the effect of BSA addition on the developed system, the immobilization time of fetuin A, and the immobilization time of PNA lectin were investigated by EIS. Since the developed system is considered to be applied for human samples like throat swabs in future, physiological human pH and body temperature were chosen as the working conditions so that all the experiments are carried out at pH 7.4 and the incubation of N was done at 37 °C.

The effect of BSA on the developed system

As is well known, BSA is generally used for the blockage of any unspecific interaction on the electrode surface, after the immobilization of the analyte. However, even for this step, there is a need to wait for a period for the completion of the attachment of BSA. In order to observe this effect, the developed influenza A biosensor was fabricated in the presence of BSA, in the absence of BSA and with the simultaneous immobilization of fetuin A. All these steps were monitored by EIS under the previously mentioned working conditions. The obtained EIS diagrams (ESI, Fig. S1†) demonstrate that for our system there is no necessity for BSA addition which means that, there is no unspecific binding during the fabrication of the developed influenza A biosensor. Also by eliminating the addition of BSA, the preparation procedure of the biosensor is shortened and as a result, the practicality of the fabrication procedure is increased. In conclusion, no BSA attachment onto the electrode surface was done for the future experiments.

Optimization of fetuin A immobilization time

Fetuin A immobilization time experiments were carried out for 15 min, 30 min, 45 min, 60 min and 90 min incubation times and the results were monitored by using EIS. The obtained EIS diagrams are presented in the ESI, Fig. S2† in addition to the Excel plots. It can be seen from Fig. S2† that the best result was obtained at 30 min. Incubation times less than 30 min resulted in a lower difference in electrode resistances, demonstrating that more time is needed probably for the exchange reactions between fetuin A amino groups and NHS to be completed. On the other hand, incubation times more than 30 min resulted in a decrease in the resistance difference that might be attributed to the separation of the non-specific bonding from the electrode surface. As a result, further experiments were conducted by using 30 min as the optimum incubation time for fetuin A.

The effect of PNA lectin immobilization time

PNA lectin immobilization time experiments were carried out for 30 min, 45 min, 60 min and 90 min immobilization times by using EIS. The obtained EIS diagrams are presented in the ESI, Fig. S3† and the Excel plots are also demonstrated in Fig. S3†. It can be seen from Fig. S3† that the best result was obtained at 60 min. Immobilization times less than 60 min resulted in a lower difference in electrode resistances demonstrating that more time is needed probably for the specific binding reactions between PNA lectin and galactose molecules to be completed. Immobilization times that lasted longer than 60 min resulted in a decrease in the resistance difference that might be attributed to the falling out of the PNA-galactose structure from the electrode surface.[11]

Analytical characteristics

After the optimization of the experimental parameters, the analytical characteristics were examined. For obtaining a calibration graph, the specific interactions between PNA lectin and galactose molecules that occur after the cleavage of N from fetuin A were monitored. When the concentration of N is increased, since more fetuin A will undergo cleavage, more galactose molecules will appear and as a result, more PNA lectin will link to the galactose ends. All these changes were monitored *via* the resistance values that were obtained from EIS measurements (Fig. 3). As can be seen from Fig. 3, the linear range and limit of detection (LOD) values which are based on the N concentration are obtained between 10^{-8} U mL^{-1} and 10^{-1} U mL^{-1} with the equations of $y = 2746x + 31.69$ ($R^2 = 0.99$) and 1×10^{-8} U mL^{-1} (1.27 ng mL^{-1}) respectively. The relative standard deviation (R.S.D) value was calculated for 10^{-5} U mL^{-1} N ($n = 3$) and found to be 3.23%. The obtained analytical characteristic values of the developed electrochemical biosensor were compared with the influenza A virus enzyme-linked immunosorbent (ELISA) assay results in the literature. These ELISA assays relied on the N activity or

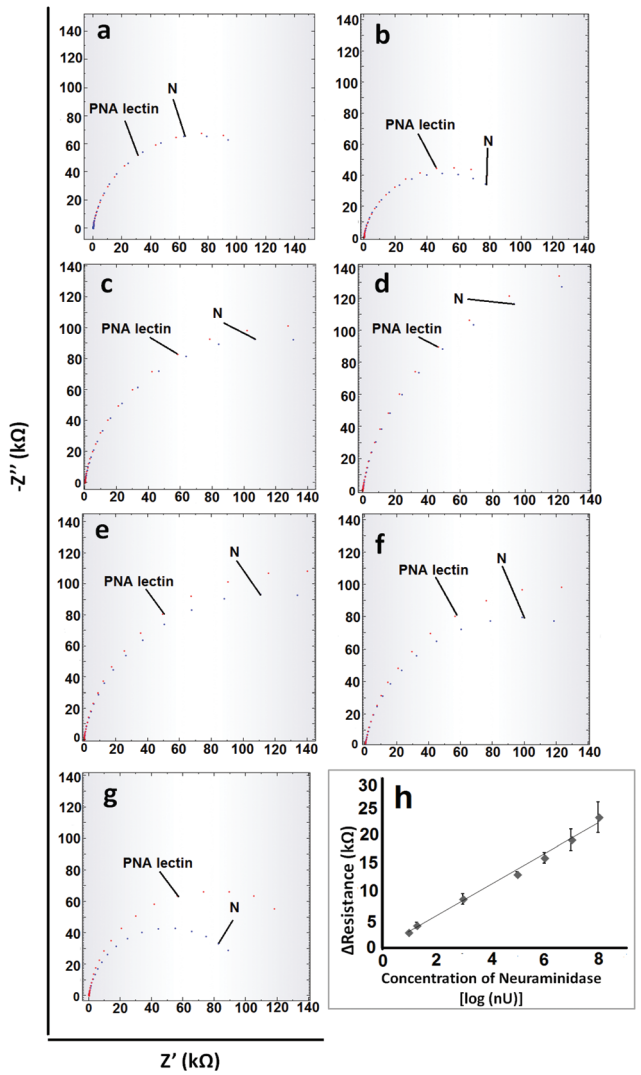

Fig. 3 Nyquist plots of different concentrations of N: (a) 10^{-8} U mL^{-1}, (b) 2×10^{-8} U mL^{-1}, (c) 10^{-6} U mL^{-1}, (d) 10^{-5} U mL^{-1}, (e) 10^{-3} U mL^{-1}, (f) 10^{-2} U mL^{-1} and (g) 10^{-1} U mL^{-1}, which were used for a calibration graph and (h) the calibration graph of the developed electrochemical influenza virus A biosensor.

antibody–antigen interactions. From these ELISA assays LOD values such as 0.7 ng mL^{-1} antigen,[53] 33 ng mL^{-1} antigen,[53] 0.5 ng mL^{-1} protein[54] and 10^2–10^3 Tissue Culture Infectious Dose 50% ($TCID_{50}$)[55] can be obtained. From these results it is clear that the developed sensor is sensitive enough. On the other hand considering its rapidity and practicality, it can be said that the developed electrochemical biosensor could definitely offer better performance.

Sample application and control studies

Evaluation of ELLA results. We developed the electrochemical influenza virus A biosensor which is based on N activity. Therefore, before we applied the developed electrochemical influenza virus A biosensor for the real H9N2 influenza type A virus detection, an ELLA experiment was carried out to demonstrate that the isolated H9N2 influenza type A virus is active according to N activity (ESI, Fig. S4†). Moreover, ELLA measurements were carried out with a control group to demonstrate that the control group is not active according to N activity. For this purpose, the ELLA results of the H9N2 virus and control groups were compared with the ELLA results of standard N. According to the ELLA results, the LOD value of N was found to be 6.52×10^{-6} U mL^{-1}. With this value we also supported the accuracy and sensitivity of the developed influenza virus A biosensor compared to the ELLA method.

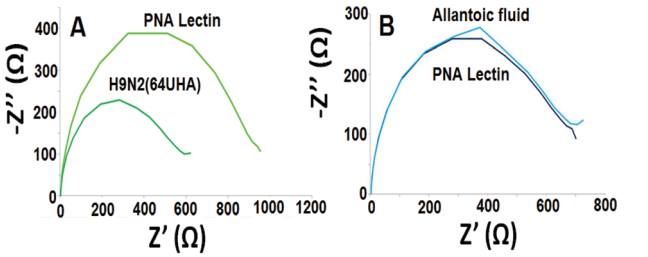

Fig. 4 Nyquist plots for (A) 64 UHA H9N2 influenza virus, and (B) the control group by using the developed electrochemical influenza virus A biosensor.

Evaluation of EIS results. The developed and optimized influenza virus A biosensor was applied for real virus detection, H9N2, that was prepared according to the procedure given in the experimental part. For this purpose, during the fabrication of the electrochemical influenza virus A biosensor, an H9N2 influenza virus A sample was used instead of N. After that, in order to determine the N activity of H9N2 influenza virus, the PNA lectin immobilization was performed.

The control study was also carried out by using an uninfected egg sample (allantoic fluid). It can be seen from Fig. 4 that the developed electrochemical influenza biosensor detects influenza A virus selectively.

Conclusions

Another novel and effective electrochemical influenza A biosensor based on graphene–Au modified Au-SPE has been developed. This work is the continuation of our previous work in which the working principle relies on the measurement of N activity.[14] From the LOD values, it is clear that with the developed electrochemical influenza A biosensor more sensitive results were obtained compared to those with the ELLA assay. We believe that, the wide linear range and sensitive results from the real influenza A sample (H9N2) analysis increase the potential of usage of our system as a point of care tool for the diagnosis of influenza virus A in the future.[56]

Conflicts of interest

There are no conflicts to declare.

Acknowledgements

The grants from The Technical and Scientific Council of Turkey (TUBITAK) Project no: 114Z654 and Tunisian Ministry of Higher Education and Scientific Research (MHESRT): Projet Tuniso-Turque 2015–2017 are gratefully acknowledged.

References

1 Y. Wu, Y. Wu, B. Tefsen, Y. Shi and G. F. Gao, *Trends Microbiol.*, 2014, **22**, 183–191.
2 N. Sriwilaijaroen and Y. Suzuki, *Proc. Japan Acad. Ser., B Phys Biol Sci.*, 2012, **88**, 226–249.
3 L. Couzens, J. Gao, K. Westgeest, M. Sandbulte, V. Lugovtsev, R. Fouchier and M. J. Eichelberger, *Virol. Methods*, 2014, **210**, 7–14.
4 D. R. Peaper and M. L. Landry, *Clin. Lab. Med.*, 2014, **34**, 365–385.
5 M. K. Abraham, J. Perkins, G. M. Vilke and C. J. Coyne, *J. Emerg. Med.*, 2016, **50**, 536–542.
6 C. M. Mair, K. Ludwig, A. Herrmann and C. Sieben, *Biochim. Biophys. Acta*, 2014, **1838**, 1153–1168.
7 J. H. Han, D. Lee, C. H. C. Chew, T. Kim and J. J. Pak, *Sens. Actuators, B*, 2016, **228**, 36–42.
8 U. Jarocka, R. Sawicka, A. Gora-Sochacka, A. Sirko, W. Zagorski-Ostoja, J. Radecki and H. Radecka, *Biosens. Bioelectron.*, 2014, **55**, 301–306.
9 S. K. Arya, P. Kongsuphol, C. C. Wong, L. J. Polla and M. K. Park, *Sens. Actuators, B*, 2014, **194**, 127–133.
10 U. Jarocka, R. Sawicka, A. Gora-Sochacka, A. Sirko, W. Dehaen, J. Radecki and H. Radecka, *Sens. Actuators, B*, 2016, **228**, 25–30.
11 L. J. Mitnaul, M. N. Matrosovich, M. R. Castrucci, A. B. Tuzikov, N. V. Bovin, D. Kobasa and Y. Kawaoka, *J. Virol.*, 2000, **74**, 6015–6020.
12 M. N. Matrosovich, T. Y. Matrosovich, T. Gray, N. A. Roberts and H. D. Klenk, *J. Virol.*, 2004, **78**, 12665–12667.
13 J. C. Dortmans, J. Dekkers, I. N. Wickramasinghe, M. H. Verheije, P. J. Rottier, F. J. Van Kuppeveld, E. De Vries and C. A. De Haan, *Sci. Rep.*, 2013, **3**, 3058.
14 U. Anik, Y. Tepeli and M. F. Diouani, *Anal. Chem.*, 2016, **88**, 6151–6153.
15 J. K. Park and J. K. Taubenberger, *ACS Infect. Dis.*, 2016, **2**, 5–7.
16 WHO. Influenza (seasonal), http://www.who.int/mediacentre/factsheets/fs211/en/ (accessed March 23, 2017).
17 H. Yu, B. J. Cowling, L. Feng, E. H. Lau, Q. Liao, T. K. Tsang, Z. Peng, P. Wu, F. Liu, V. J. Fang, H. Zhang, M. Li, L. Zeng, Z. Xu, Z. Li, H. Luo, Q. Li, Z. Feng, B. Cao, W. Yang, J. T. Wu, Y. Wang and G. M. Leung, *Lancet*, 2013, **382**, 138–145.
18 L. Krejcova, D. Hynek, V. Adam, J. Hubalek and R. Kizek, *Int. J. Electrochem. Sci.*, 2012, **7**, 10779–10801.
19 J. Bell, A. Bonner, D. M. Cohen, R. Birkhahn, R. Yogev, W. Triner, J. Cohen, E. Palavecino and R. Selvarangan, *J. Clin. Virol.*, 2014, **61**, 81–86.
20 K. Leirs, P. T. Kumar, D. Decrop, E. Perez-Ruiz, P. Leblebici, B. V. Kelst, G. Compernolle, H. Meeuws, L. V. Wesenbeeck, O. Lagatie, L. Stuyver, A. Gils, J. Lammertyn and D. Spasic, *Anal. Chem.*, 2016, **80**, 8450–8458.
21 C. H. Cho, M. K. Woo, J. Y. Kima, S. Cheong, C.-K. Lee, S. A. An, C. S. Lim and W. J. Kim, *J. Virol. Methods*, 2013, **187**, 51–56.
22 L. Chen, Y. Tian, S. Chen and O. Liesenfield, *Eur. J. Microbiol. Immunol.*, 2015, **5**, 236–245.
23 B. Hazelton, T. Gray, J. Ho, V. M. Ratnamohan, D. E. Dwyer and J. Kok, *Influenza Other Respir. Viruses*, 2015, **9**, 151–154.
24 D. E. Sutter, S. A. Worthy, D. M. Hensley, A. M. Maranich, D. M. Dolan, G. W. Fischer and L. T. Daum, *J. Med. Virol.*, 2012, **84**, 1699–1702.
25 M. Santhiago, M. Strauss, M. P. Pereira, A. S. Chagas and C. C. B. Bufon, *ACS Appl. Mater. Interfaces*, 2017, **9**, 11959–11966.
26 C. Batchelor-McAuley, E. J. F. Dickinson, N. V. Rees, K. E. Toghill and R. G. Compton, *Anal. Chem.*, 2012, **84**, 669–684.
27 J. E. Frew and H. A. O. Hill, *Anal. Chem.*, 1987, **59**, 933A–944A.
28 Y. Xu, L. Liu, Z. Wang and Z. Dai, *ACS Appl. Mater. Interfaces*, 2016, **8**, 18669–18674.
29 U. Anik, Med. Biosens. for POC Appl., in *Electrochemical medical biosensors for POC applications*, ed. R. J. Narayan, Woodhead Publishing, 2016, ch. 12, vol. 2017, pp. 275–292.
30 C. Zhu, G. Yang, H. Li, D. Du and Y. Lin, *Anal. Chem.*, 2015, **87**, 230–249.
31 J. Wang, *Analyst*, 2005, **130**, 421–426.
32 Li, X. Su and Y. Lu, *Analyst*, 2015, **140**, 2916–2943.
33 J. N. Tiwari, V. Vij, K. C. Kemp and K. S. Kim, *ACS Nano*, 2016, **10**, 46–80.
34 Y. Shao, J. Wang, H. Wu, J. Liu, I. A. Aksay and Y. Lin, *Electroanalysis*, 2010, **22**, 1027–1036.
35 S. Wu, Q. He, C. Tan, Y. Wang and H. Zhang, *Small*, 2013, **9**, 1160–1172.
36 X. Gan and H. Zhao, *Sens. Mater.*, 2015, **27**, 191–215.
37 C. Xu, X. Wang and J. Zhu, *J. Phys. Chem. C*, 2008, **112**, 19841–19845.
38 Y. Tepeli and U. Anik, *Electroanalysis*, 2016, **28**, 3048–3054.
39 Z. Zhang, L. Luo, L. Zhu, Y. Ding, D. Deng and Z. Wang, *Analyst*, 2013, **138**, 5365–5370.
40 S. Aslan and U. Anik, *Microchim. Acta*, 2016, **183**, 73–81.
41 S. C. Sultan and U. Anik, *Talanta*, 2014, **129**, 523–528.
42 M. Giovanni, H. L. Poh, A. Ambrosi, G. Zhao, Z. Sofer, F. Sanek, B. Khezri, R. D. Webster and M. Pumera, *Nanoscale*, 2012, **4**, 5002–5008.
43 C. Tan, X. Huang and H. Zhang, *Mater. Today*, 2013, **16**, 29–36.
44 M. F. Diouani, S. Helali, I. Hafaid, W. M. Hassen, M. A. Snoussi, A. Ghram, N. Jaffrezic-Renault and A. Abdelghani, *Mater. Sci. Eng., C*, 2008, **28**, 580–583.
45 T. L. Kamikawa, M. G. Mikolajczyk, M. Kennedy, P. Zhang, W. Wang, D. E. Scott and E. C. Alocilja, *Biosens. Bioelectron.*, 2010, **26**, 1346–1352.

46 M. Veerapandian, R. Hunter and S. Neethirajan, *Talanta*, 2016, **155**, 250–257.
47 J. Huang, Z. Xie, Z. Xie, S. Luo, L. Xie, L. Huang, Q. Fan, Y. Zhang, S. Wang and T. Zeng, *Anal. Chim. Acta*, 2016, **913**, 121–127.
48 Z. Wu, C. H. Zhou, J. J. Chen, C. Xiong, Z. Chen, D. W. Pang and Z. L. Zhang, *Biosens. Bioelectron.*, 2015, **68**, 586–592.
49 W. S. J. Hummers and R. J. Offeman, *Am. Chem. Soc.*, 1958, **80**, 1339.
50 D. Li, M. B. Mgller, S. Gilje, R. B. Kaner and G. G. Wallace, *Nat. Nanotechnol.*, 2008, **3**, 101–105.
51 S. Stankovich, D. A. Dikin, G. H. Dommett, K. M. Kohlhaas, E. J. Zimney, E. A. Stach, R. D. Piner, S. T. Nguyen and R. S. Ruoff, *Nature*, 2006, **442**, 282–286.
52 Y. Tepeli and U. Anik, *Electrochem. Commun.*, 2015, **57**, 31–34.
53 W. Honquan, I. Sultana, L. K. Couzens and S. Mindaye, *J. Virol. Methods*, 2017, **244**, 23–28.
54 G. Edevag, M. Eriksson and M. Granström, *J. Biol. Stand.*, 1986, **14**, 223–230.
55 S. Velumani, Q. Du, B. J. Fenner, M. Prabakaran, L. C. Wee, L. Y. Nuo and J. Kwang, *J. Virol. Methods*, 2008, **147**, 219–225.
56 Y. Tepeli and U. Anik, *Sens. Actuators, B*, 2018, **254**, 377–384.